NASA TECHNICAL NOTE

NASA TN D-7424

NASA TN D-7424

APPLICATION OF BOUNDARY INTEGRAL METHOD TO ELASTIC ANALYSIS OF V-NOTCHED BEAMS

by Walter Rzasnicki, Alexander Mendelson, and Lynn U. Albers

Lewis Research Center
Cleveland, Ohio 44135

NATIONAL AERONAUTICS AND SPACE ADMINISTRATION • WASHINGTON, D. C. • OCTOBER 1973

1. Report No.	2. Government Accession No.	3. Recipient's Catalog No.
NASA TN D-7424		

4. Title and Subtitle	5. Report Date
APPLICATION OF BOUNDARY INTEGRAL METHOD TO ELASTIC ANALYSIS OF V-NOTCHED BEAMS	October 1973
	6. Performing Organization Code
7. Author(s)	8. Performing Organization Report No.
Walter Rzasnicki, Alexander Mendelson, and Lynn U. Albers	E-7156
	10. Work Unit No.
9. Performing Organization Name and Address	501-21
Lewis Research Center National Aeronautics and Space Administration Cleveland, Ohio 44135	11. Contract or Grant No.
	13. Type of Report and Period Covered
12. Sponsoring Agency Name and Address	Technical Note
National Aeronautics and Space Administration Washington, D.C. 20546	14. Sponsoring Agency Code

15. Supplementary Notes

16. Abstract

A semidirect boundary integral method, using Airy's stress function and its derivatives in Green's boundary integral formula, is used to obtain an accurate numerical solution for elastic stress and strain fields in V-notched beams in pure bending. The proper choice of nodal spacing on the boundary is shown to be necessary to achieve an accurate stress field in the vicinity of the tip of the notch. Excellent agreement is obtained with the results of the collocation method of solution.

17. Key Words (Suggested by Author(s))	18. Distribution Statement
Fracture mechanics; Stress-intensity factor; V-notch; Boundary integrals; Elasticity	Unclassified - unlimited

19. Security Classif. (of this report)	20. Security Classif. (of this page)	21. No. of Pages	22. Price*
Unclassified	Unclassified	28	Domestic, $3.00 Foreign, $5.50

* For sale by the National Technical Information Service, Springfield, Virginia 22151

APPLICATION OF BOUNDARY INTEGRAL METHOD TO ELASTIC ANALYSIS OF V-NOTCHED BEAMS

by Walter Rzasnicki, Alexander Mendelson, and Lynn U. Albers

Lewis Research Center

SUMMARY

A semidirect boundary integral method, using Airy's stress function and its derivatives in Green's boundary integral formula, is used to obtain an accurate numerical solution for elastic stress and strain fields in V-notched beams in pure bending. The proper choice of nodal spacing on the boundary is shown to be necessary to achieve an accurate stress field in the vicinity of the tip of the notch. Excellent agreement is obtained with the results of the collocation method of solution.

INTRODUCTION

Knowledge of the stress distribution in the neighborhood of a singularity, such as the tip of a V-notch in a beam loaded in tension or bending, is of fundamental importance in evaluating the resistance to fracture of structural materials. Elastic solutions to various geometries have been obtained by a number of different methods. Among the more effective ones, are the complex variable method (ref. 1), collocation method (ref. 2), and finite element method (ref. 3). However, the first two of these methods are not general enough nor readily adaptable to three-dimensional or elastoplastic problems. And the finite element method requires solutions of large sets of equations and fails to give sufficiently fine resolution in the vicinity of crack tips.

The recently developed boundary integral methods (ref. 4) offer an attractive alternative to other methods of analysis. These methods have a number of advantages which may be listed as follows:

(1) They obviate the need for conformal mapping.

(2) Mixed boundary value problems are handled with ease.

(3) Stresses and displacements are obtained directly without need for numerical differentiation.

(4) No special considerations are needed for multiply connected regions.

(5) The internal stresses and/or displacements are calculated only where and when needed.

(6) The extension to three-dimensional problems is direct.

(7) Nodal points are needed only on the boundary instead of throughout the interior as required by finite element methods.

The last point, which is probably the most important one, is illustrated in figure 1. For the finite element method, the whole region must be covered by a grid producing a large number of nodal points and corresponding unknowns. Thus a large number of simultaneous equations must be solved. For the boundary integral methods, nodal points are taken only on the boundary, resulting in a much smaller number of unknowns.

The object of this report is to present a solution to the elastic problem of a V-notched beam in pure bending using one of the boundary integral methods described in reference 4. A necessary part of this solution is the strategy by which the nodal spacing on the boundary is chosen to achieve stable and accurate solutions. It is intended to use the spacing which gives good elastic results in the extension of the method to the more interesting and complicated elastoplastic problem, which will be discussed in a subsequent report.

SYMBOLS

a	notch depth
$\tilde{a}$	dimensionless notch depth, a/w
$a_{ij}, b_{ij}, c_{ij}, d_{ij}, e_{ij}, f_{ij}$	coefficients in boundary equations
$A_{ij}, B_{ij}, C_{ij}, D_{ij}, E_{ij}, F_{ij}, G_{ij}, H_{ij}, I_{ij}, K_{ij}$	coefficients in stress equations
C	boundary contour
E	Young's modulus of elasticity
J	value of Rice's contour integral
K_I	stress intensity factor at notch tip for mode I crack opening
L	half length of beam

n	order of stress singularity in vicinity of tip of notch
$\bar{n}, \bar{s}$	unit vectors normal and tangent to contour C
$P(x, y)$	point on contour C or in region R
$q(\xi, \eta)$	point on contour C
$\tilde{q}$	dimensionless load, σ_{max}/σ_0
R	planar region bounded by closed contour C
r_{ij}	distance between two points having coordinates $(x, y)_i$ and $(\xi, \eta)_j$
r, θ	polar coordinate directions
s	length measured along contour C
T_i	stress vector active along boundary
u_i	displacement vector
u_y	displacement in y-direction
$u(x, y), v(x, y)$	arbitrary continuous functions
$W(\epsilon)$	strain energy density
w	width of beam
x, y, z	rectangular Cartesian coordinate directions
$\tilde{x}, \tilde{y}$	dimensionless rectangular Cartesian coordinate directions, x/w, y/w
α	notch angle, deg
δ_{ij}	Kronecker delta
ϵ_{ij}	strain tensor
Γ	arbitrary contour surrounding crack tip
μ	Poisson's ratio
ξ, η	rectangular Cartesian coordinate directions
ρ	function of r, $\rho = r^2 \ln r$
σ_{ij}	stress tensor
σ_{max}	maximum nominal bending stress
$\sigma_x, \sigma_y, \sigma_z, \sigma_{xy}$	components of stress tensor in Cartesian coordinates
σ_0	tensile yield stress
Φ	function of Airy stress function, $\Phi = \nabla^2 \varphi$
φ	Airy stress function

∇^2 Laplace's operator, $\partial^2/\partial x^2 + \partial^2/\partial y^2$

∇^4 biharmonic operator, $\partial^4/\partial x^4 + 2\,\partial^4/\partial x^2 \partial y^2 + \partial^4/\partial y^4$

Subscripts:

i, j, k integers

Superscripts:

~ dimensionless quantity

' derivative in outward normal direction, $\partial/\partial n$

ANALYSIS

The Integral Equation Method

The problem of determining the state of stress in a plane elastostatic problem can be reduced to solving a homogeneous biharmonic equation

$$\nabla^4 \varphi(x, y) = 0 \tag{1}$$

subject to appropriate boundary conditions, where $\varphi(x, y)$ is the Airy stress function and the components of the stress tensor, in Cartesian coordinates, are

$$\sigma_x = \frac{\partial^2 \varphi}{\partial y^2}, \qquad \sigma_y = \frac{\partial^2 \varphi}{\partial x^2}, \qquad \sigma_{xy} = -\frac{\partial^2 \varphi}{\partial x \partial y} \tag{2}$$

For the problem under consideration (fig. 2) the stress function $\varphi(x, y)$ and its outward normal derivative $\partial\varphi/\partial n$ must satisfy the following boundary conditions (ref. 5):

along boundary OA and OA':

$$\varphi(x, y) = 0; \frac{\partial \varphi}{\partial n} = 0$$

along boundary AB and A'B':

$$\varphi(x, y) = 0; \frac{\partial \varphi}{\partial n} = 0$$

along boundary BC and B'C':

$$\varphi(x, y) = -\frac{\sigma_{max}}{w}\left(\frac{x^3}{3} + ax^2 + a^2x + \frac{a^3}{3}\right) + \sigma_{max}\left(\frac{x^2}{2} + ax + \frac{a^2}{2}\right); \frac{\partial \varphi}{\partial n} = 0 \qquad (3)$$

along boundary CD and C'D:

$$\varphi(x, y) = \frac{\sigma_{max} w^2}{6}; \frac{\partial \varphi}{\partial n} = 0$$

The method of solution utilizes Green's second theorem to reduce the homogeneous biharmonic equation (1) to two coupled, Fredholm type, integral equations, which must satisfy the specified boundary conditions.

Green's second theorem states

$$\iint_R (u\nabla^2 v - v\nabla^2 u)\, dx\, dy = \int_C \left(u \frac{\partial v}{\partial n} - v \frac{\partial u}{\partial n}\right) ds \qquad (4)$$

where the arbitrary functions $u(x, y)$ and $v(x, y)$ and their derivatives of first and second order are continuous in the simply connected region R, bounded by a sectionally smooth curve C. The notation employed is depicted in figure 3.

If we let

$$u = \nabla^2 \varphi \qquad (5)$$

then it follows, that

$$\iint_R (\varphi \nabla^4 v - v\nabla^4 \varphi)\, dx\, dy = \int_C \left[\varphi \frac{\partial}{\partial n}(\nabla^2 v) - \frac{\partial \varphi}{\partial n} \nabla^2 v + \nabla^2 \varphi \frac{\partial v}{\partial n} - v \frac{\partial}{\partial n}(\nabla^2 \varphi)\right] ds \qquad (6)$$

Let us introduce the function $\Phi(x, y)$ such that

$$\Phi \equiv \nabla^2 \varphi \tag{7}$$

Substituting equation (7) into equation (1) yields

$$\nabla^2 \Phi(x, y) = 0 \tag{8}$$

Let $r(x, y; \xi, \eta)$ be the distance between any two points $P(x, y)$ and $q(\xi, \eta)$ in the region R, as shown in figure 3, such that $P \subset R + C$ and $q \subset C$.

Substituting relations (5), (7), and (8) into Green's second theorem, equation (4), choosing first, $v = \ln r$ (the fundamental solution of $\nabla^2 v = 0$) and taking into account the singularity at $r = 0$ (ref. 5) results in

$$2\pi\Phi(x, y) = \int_C \left[\Phi \frac{\partial}{\partial n} (\ln r) - \frac{\partial \Phi}{\partial n} \ln r\right] ds \qquad \text{for} \quad P \subset R \tag{9}$$

and

$$\pi\Phi(x, y) = \int_C \left[\Phi \frac{\partial}{\partial n} (\ln r) - \frac{\partial \Phi}{\partial n} \ln r\right] ds \qquad \text{for} \quad P \subset C \tag{10}$$

Combining equation (6) with equations (1) and (7) and choosing this time $v \equiv \rho = r^2 \ln r$, and taking into account the singularity at $r = 0$, we obtain (ref. 6)

$$8\pi\varphi(x, y) = \int_C \left[\varphi \frac{\partial}{\partial n} (\nabla^2 \rho) - \frac{\partial \varphi}{\partial n} \nabla^2 \rho + \Phi \frac{\partial \rho}{\partial n} - \frac{\partial \Phi}{\partial n} \rho\right] ds \qquad \text{for} \quad P \subset R \tag{11}$$

and

$$4\pi\varphi(x, y) = \int_C \left[\varphi \frac{\partial}{\partial n} (\nabla^2 \rho) - \frac{\partial \varphi}{\partial n} \nabla^2 \rho + \Phi \frac{\partial \rho}{\partial n} - \frac{\partial \Phi}{\partial n} \rho\right] ds \qquad \text{for} \quad P \subset C \tag{12}$$

Equation (11) would give us directly a solution to the biharmonic equation (1) provided the functions $\varphi(x, y)$, $\partial\varphi(x, y)/\partial n$, $\nabla^2\varphi(x, y)$, and $\partial\left[\nabla^2\varphi(x, y)\right]/\partial n$ were known on the boundary C.

However, only the stress function φ and its outward normal derivative $\partial\varphi/\partial n$

are specified on the boundary. The values of $\nabla^2\varphi \equiv \Phi$ and $\partial(\nabla^2\varphi)/\partial n \equiv \partial\Phi/\partial n$ on the boundary must be compatible with these boundary conditions. To assure this compatibility, we have to solve the system of coupled integral equations (10) and (12), which contain the unknown functions Φ and $\partial\Phi/\partial n$.

Once the values of Φ and $\partial\Phi/\partial n$ on the boundary C of the region R are known we can proceed with the calculation of the stress field in the region R utilizing equations (11) and (2).

Numerical Procedures

Solution of the integral equations. - Since it is generally impossible to solve the system of coupled integral equations analytically, a numerical method is utilized in which the integral equations (10) and (12) are replaced by a system of simultaneous algebraic equations.

For simplicity of notation, let us denote the normal derivatives by prime superscripts.

Let us assume that the function Φ and its normal derivative Φ' are piece-wise constant on the boundary C. We can divide the boundary into n intervals, not necessarily equal, numbered consecutively in the direction of increasing s. The center of each interval is designated as a node and assigned the constant values of Φ_i and Φ_i'. The arrangements of boundary subdivisions is shown in figure 4.

Using these assumptions, equations (10) and (12) can be replaced by a system of 2n simultaneous algebraic equations with 2n unknowns, that is, Φ_i and Φ_i'

$$\left.\begin{aligned} \pi\Phi_i &= \sum_{j=1}^{n} (a_{ij}\Phi_j + b_{ij}\Phi_j') \\ 4\pi\varphi_i &= \sum_{j=1}^{n} (c_{ij}\Phi_j + d_{ij}\Phi_j' + e_{ij}\varphi_j + f_{ij}\varphi_j') \end{aligned}\right\} \tag{13}$$

where i = 1, 2, 3 . . . n. The coefficients appearing in the boundary equations (13) are defined by the following relations:

$$
\left.
\begin{aligned}
a_{ij} &= \int_j (\ln r_{ij})' \, ds \\
b_{ij} &= -\int_j \ln r_{ij} \, ds \\
c_{ij} &= \int_j \rho'_{ij} \, ds \\
d_{ij} &= -\int_j \rho_{ij} \, ds \\
e_{ij} &= \int_j (\nabla^2 \rho_{ij})' \, ds \\
f_{ij} &= -\int_j \nabla^2 \rho_{ij} \, ds
\end{aligned}
\right\} \tag{14}
$$

where integration is taken over the j^{th} interval, and r_{ij} is the distance from i^{th} node to any point in the j^{th} interval. The normal derivatives in equation (14) are taken on the j^{th} interval.

The coefficients given by equations (14) can be evaluated by Simpson's rule for $i \neq j$, and analytically for $i = j$. For the boundary intervals which can be represented by straight lines an analytical solution is possible for all the coefficients.

Equations (13) expressed in matrix form become

$$
\begin{bmatrix}
\underset{n \times n}{[a_{ij} - \delta_{ij}\pi]} & \underset{n \times n}{[b_{ij}]} \\
\underset{n \times n}{[c_{ij}]} & \underset{n \times n}{[d_{ij}]}
\end{bmatrix}
\begin{Bmatrix}
\underset{n \times 1}{[\Phi_j]} \\
\underset{n \times 1}{[\Phi'_j]}
\end{Bmatrix}
= -
\begin{bmatrix}
\underset{n \times n}{[0]} & \underset{n \times n}{[0]} \\
\underset{n \times n}{[e_{ij} - \delta_{ij} 4\pi]} & \underset{n \times n}{[f_{ij}]}
\end{bmatrix}
\begin{Bmatrix}
\underset{n \times 1}{[\varphi_j]} \\
\underset{n \times 1}{[\varphi'_j]}
\end{Bmatrix}
\tag{15}
$$

Thus, the problem is reduced to the solution of the following matrix system:

$$
[B]\{X\} = \{R\} \tag{16}
$$

where $[B]$ is a $2n \times 2n$ matrix and $\{X\}$ and $\{R\}$ are $2n \times 1$ column matrices.

To calculate stresses for any point in the region R from the stress function (11), we need not perform any numerical differentiation of the stress function. Once Φ and Φ' are known on the boundary we can differentiate under the integral sign in this equation and then obtain stresses by the same type of numerical integration as in equations (13). Applying equations (2) to equation (11) and using notations of equations (14) yields the stress equations

$$\left.\begin{aligned} 8\pi\sigma_x(x,y)_i &= \sum_{j=1}^{n} (A_{ij}\varphi_j + B_{ij}\varphi'_j + C_{ij}\Phi_j + D_{ij}\Phi'_j) \\ 8\pi\sigma_y(x,y)_i &= \sum_{j=1}^{n} (-A_{ij}\varphi_j - B_{ij}\varphi'_j + E_{ij}\Phi_j + F_{ij}\Phi'_j) \\ -8\pi\sigma_{xy}(x,y)_i &= \sum_{j=1}^{n} (G_{ij}\varphi_j + H_{ij}\varphi'_j + I_{ij}\Phi_j + K_{ij}\Phi'_j) \end{aligned}\right\} \qquad (17)$$

where i refers to any point in the stress field, and the coefficients A_{ij}, B_{ij}, C_{ij}, D_{ij}, E_{ij}, F_{ij}, G_{ij}, H_{ij}, I_{ij}, and K_{ij} are obtained by appropriate differentiation under the integral sign of the coefficients given by equations (14), and are listed in the appendix.

The stress function φ is not constant on the loaded boundaries BC and B'C'. The assumption that it is piece-wise constant may lead to appreciable errors in the numerical results. To overcome this difficulty, the summations given in equations (13) and (17) for intervals lying on the loaded boundaries and involving the stress function are replaced by direct integration.

Boundary interval size. - The number of nodal points prescribed for the boundary is theoretically unlimited. However, computer storage capacity for the computer used and the difficulties associated with inversion of large matrices limited the order of the coefficient matrix $[B]$ of equation (16) used herein to 140.

Because of geometric and loading symmetry about the x axis it is possible to reduce the number of unknowns. For $2n$ total number of nodal points the number of equations and unknowns, Φ_i and Φ'_i, is reduced from $4n$ to $2n$. Additional reduction in the number of unknowns is accomplished by taking into consideration the St. Venant's effect at the loaded boundaries. By definition

$$\Phi_j \equiv \nabla^2\varphi_j = \sigma_{x_j} + \sigma_{y_j}$$

Since, near the loaded boundaries BC and B'C', σ_{x_j} can be assumed to be essentially zero if $\tilde{L} \geq 1.2$ (ref. 2), then it follows that

$$\left.\begin{aligned} \Phi_j &= \sigma_{y_j} \\ \Phi_j' \equiv \frac{\partial \sigma_{y_j}}{\partial n} &= 0 \end{aligned}\right\} \tag{18}$$

Thus on the boundaries BC and B'C', Φ_j and Φ_j' are known.

The arrangement of boundary subdivisions and nodal points is shown in figure 5. Note that the corner points are always designated as interval points, never as nodal points, thus eliminating discontinuous functions from the numerical analysis.

Since the vicinity of the crack tip is of greatest interest, a fine nodal spacing along the notch was chosen. To reduce the error introduced by the change in the interval size (ref. 7) around boundary points A and A' and at the same time to obtain fine resolution at the tip of the notch, the boundary along the notch was divided into a number of intervals progressively decreasing in length. The rate of change in the interval length and the resulting length of the smallest interval was found to have a great influence on the stress field in the vicinity of the tip of the notch.

Each of the boundaries AB, A'B', DC and DC' was divided into 5 intervals of equal length. Each of the boundaries BC and B'C' were assigned values of Φ_j and Φ_j', given by equations (18), at 15 uniformly spaced nodal points. To complete the boundary nodal arrangement, 60 nodal points were taken along each of the boundaries along the notch. The rate of change in the interval's length along these boundaries was optimized for all cases by the method illustrated in figure 6 for the case of a specimen with a 10° edge notch and $a/w = 0.3$. The dimensionless y-directional stresses at three locations below the tip of the notch were plotted as a function of tapering ratio, that is, the ratio of the lengths of two consecutive boundary intervals. Note that the stresses far enough from the tip were insensitive to changes of the taper. The general pattern was that the stress converges smoothly to its correct value as the tapering ratio increases until at a certain point it starts to oscillate erratically. This behavior is caused by the violent oscillations in Φ and Φ' near the tip of the notch that occur when the minimum interval length becomes too small.

This result suggests the following strategy in choosing the optimum tapering ratio for a given number of boundary intervals along the notch:

(1) Plot the x-directional or y-directional stresses at several locations below the tip of the notch, where good resolution of stresses is desired, for a sequence of tapering ratios.

(2) Start with a ratio of 1.00 and increase it uniformly. Continue plotting these curves from the smooth monotonic regime into the region where the variation becomes erratic. Pick as an optimum ratio the largest one that is in the smooth regime for all curves.

For the case of a 10° edge notch and an $a/w = 0.3$, an optimum tapering ratio of 1.09 is associated with the smallest dimensionless interval length of approximately 0.00015. For the other cases considered, optimum ratios were found to be in the range of 1.08 to 1.10. The resulting smallest dimensionless boundary interval length varied from 0.0001 to 0.0002.

The nodal arrangement shown in figure 5 was used for all cases considered, resulting in a set of 140 equations containing 140 unknowns, that is, Φ_i and Φ_i', $i = 1, 2, 3, \ldots, 70$.

The numerical calculations were performed on an IBM 7094 digital computer using single-precision arithmetic. The matrix system given by equation (16) was solved using the modified Gauss elimination method, which utilizes pivoting and forward and backward substitutions.

RESULTS AND DISCUSSION

The computations were performed for cases of 10°, 30°, and 60° notch angles and varying notch depths. Selected results were also obtained for a 3° notch angle. Figures 7 to 9 show x-directional and y-directional stress distribution as a function of distance from the tip of the notch. The results are compared with stress values obtained by the boundary collocation technique reported by Gross (ref. 2) and are found to be in excellent agreement. Table I contains selected results of these stress computations.

As expected, the stresses approach infinity near the tip of the notch. The square root singularity associated with the crack changes from 0.500 to approximately 0.488 for a 60° notch angle as shown in table II. The order of stress singularity computed herein is compared with results given by Gross and Mendelson (ref. 8) and excellent agreement is obtained.

The stress intensity factor K_I under mode I notch displacement is defined (ref. 2), in terms of the coordinate system shown in figure 2, as follows:

$$K_I = \lim_{r \to 0} \sqrt{2\pi}\, r^n\, \sigma_y(r, \theta)\Big|_{\theta=0} \tag{19}$$

From the known stress field in the vicinity of the tip of the notch the order of stress singularity n in equation (19) can be determined by plotting $\ln \sigma_y$ against $\ln r$, and

obtaining a least-squares fit of a straight line through the plotted points. The slope of the line gives n.

Once the order of stress singularity is found, a plot of the function of r in equation (19) as $r \to 0$ yields the stress intensity factor K_I. Figure 10 shows the variation of the dimensionless stress intensity factor $\tilde{K}_I$ with notch depth for a 10^o notch as compared to the analytical solution obtained by Gross and Mendelson (ref. 8). These analytical results generally give values higher by approximately 1 percent.

Figure 11 shows the dimensionless elastic plane-stress displacements at the edge of the notch as a function of notch depth. The displacements were obtained by numerical integration of relation (22) along straight line paths. The comparison is made with available results by Gross (ref. 2) and are found to be in very good agreement.

Finally, the relations between path independent Rice's integral J and the stress intensity factor K_I were checked. These relations were given by Rice (ref. 9) for a linear elastic body in the following form:

$$J = \frac{1 - \mu^2}{E} K_I^2 \quad \text{(for plane strain)} \tag{20a}$$

$$J = \frac{1}{E} K_I^2 \quad \text{(for plane stress)} \tag{20b}$$

where J is defined as

$$J = \int_\Gamma \left[W(\epsilon)\, dy - T_i \frac{\partial u_i}{\partial x}\, ds \right] \tag{21}$$

Here Γ is an arbitrary curve surrounding the notch tip. The integral is evaluated in a counterclockwise sense, starting from the notch surface. Strain energy density is defined as

$$W(\epsilon_{mn}) = \int_0^{\epsilon_{mn}} \sigma_{ij}\, d\epsilon_{ij}$$

and the traction vector is

$$T_i = \sigma_{ij} n_j$$

while u_i is a displacement vector defined in terms of strain tensor as

$$\epsilon_{ij} = \frac{1}{2}(u_{i,j} + u_{j,i}) \tag{22}$$

Equations (20) allow one to evaluate the stress intensity factors without detailed knowledge of the stress field very near the notch tip.

For the plane-stress case, the comparison between J values obtained by numerical integration of relation (21) and by use of equation (20b) is shown in table III.

CONCLUSIONS

The results obtained for the elastic stress analysis of V-notched beams subjected to pure bending compared very well with the collocation method of solution. The boundary integral method appears to be well suited for the solution of problems with geometric singularities. The dependence of the accuracy of the stress field in the vicinity of notch tip on the choice of nodal spacing has been demonstrated. The strategy of making this choice has been shown to be successful by comparison to results obtained by the collocation method of solution. The experience gained from those studies can now be utilized in performing the more complicated elastoplastic calculations.

Lewis Research Center,
National Aeronautics and Space Administration,
Cleveland, Ohio, July 20, 1973,
501-21.

APPENDIX - COEFFICIENTS OF THE STRESS EQUATIONS

The coefficients appearing in stress equations (17) are given by the following relations:

$$A_{ij} = \frac{\partial^2}{\partial y^2}(e_{ij}) = 4 \int_j \frac{\partial}{\partial n} \left\{ \frac{(x_i - \xi)^2 - (y_i - \eta)^2}{\left[(x_i - \xi)^2 + (y_i - \eta)^2\right]^2} \right\} ds$$

$$B_{ij} = \frac{\partial^2}{\partial y^2}(f_{ij}) = 4 \int_j \frac{(y_i - \eta)^2 - (x_i - \xi)^2}{\left[(x_i - \xi)^2 + (y_i - \eta)^2\right]^2} ds$$

$$C_{ij} = \frac{\partial^2}{\partial y^2}(c_{ij}) = \int_j \frac{\partial}{\partial n} \left\{ \ln \left[(x_i - \xi)^2 + (y_i - \eta)^2\right] + \frac{2(y_i - \eta)^2}{(x_i - \xi)^2 + (y_i - \eta)^2} \right\} ds$$

$$D_{ij} = \frac{\partial^2}{\partial y^2}(d_{ij}) = - \int_j \left\{ \ln \left[(x_i - \xi)^2 + (y_i - \eta)^2\right] + \frac{2(y_i - \eta)^2}{(x_i - \xi)^2 + (y_i - \eta)^2} + 1 \right\} ds$$

$$E_{ij} = \frac{\partial^2}{\partial x^2}(c_{ij}) = \int_j \frac{\partial}{\partial n} \left\{ \ln \left[(x_i - \xi)^2 + (y_i - \eta)^2\right] + \frac{2(x_i - \xi)^2}{(x_i - \xi)^2 + (y_i - \eta)^2} \right\} ds$$

$$F_{ij} = \frac{\partial^2}{\partial x^2}(d_{ij}) = - \int_j \left\{ \ln \left[(x_i - \xi)^2 + (y_i - \eta)^2\right] + \frac{2(x_i - \xi)^2}{(x_i - \xi)^2 + (y_i - \eta)^2} + 1 \right\} ds$$

$$G_{ij} = \frac{\partial^2}{\partial x\, \partial y}(e_{ij}) = -8 \int_j \frac{\partial}{\partial n}\left\{\frac{(x_i - \xi)(y_i - \eta)}{\left[(x_i - \xi)^2 + (y_i - \eta)^2\right]^2}\right\} ds$$

$$H_{ij} = \frac{\partial^2}{\partial x\, \partial y}(f_{ij}) = 8 \int_j \frac{(x_i - \xi)(y_i - \eta)}{\left[(x_i - \xi)^2 + (y_i - \eta)^2\right]^2} ds$$

$$I_{ij} = \frac{\partial^2}{\partial x\, \partial y}(c_{ij}) = 2 \int_j \frac{\partial}{\partial n}\left[\frac{(x_i - \xi)(y_i - \eta)}{(x_i - \xi)^2 + (y_i - \eta)^2}\right] ds$$

$$K_{ij} = \frac{\partial^2}{\partial x\, \partial y}(d_{ij}) = -2 \int_j \frac{(x_i - \xi)(y_i - \eta)}{(x_i - \xi)^2 + (y_i - \eta)^2} ds$$

The evaluation of these integrals is given in reference 5.

REFERENCES

1. Bowie, O. L.: Rectangular Tensile Sheet with Symmetric Edge Cracks. J. Appl. Mech., vol. 86, no. 2, June 1964, pp. 208-212.

2. Gross, Bernard: Some Plane Problem Elastostatic Solutions for Plates Having a V-Notch. Ph. D. Thesis, Case Western Reserve Univ., 1970.

3. Hays, David James: Some Applications of Elastic-Plastic Analysis to Fracture Mechanics. Ph. D. Thesis, Imperial College of Science and Technology, Univ. London, 1970.

4. Mendelson, Alexander: Boundary Integral Methods in Elasticity and Plasticity. NASA TN D-7418, 1973.

5. Rzasnicki, Walter: Plane Elasto-Plastic Analysis of V-Notched Plate Under Bending by Boundary Integral Equation Method. Ph. D. Thesis, Univ. Toledo, 1973.

6. Collatz, Lothar: The Numerical Treatment of Differential Equations. Third ed. Springer-Verlag, 1960.

7. Walker, George E., Jr.: A Study of the Applicability of the Method of Potential to Inclusions of Various Shapes in Two- and Three-Dimensional Elastic and Thermoelastic Stress Fields. Ph. D. Thesis, Univ. Washington, 1969.

8. Gross, Bernard; and Mendelson, Alexander: Plane Elastostatic Analysis of V-Notched Plates. NASA TN D-6040, 1970.

9. Rice, James R.: A Path Independent Integral and the Approximate Analysis of Strain Concentration by Notches and Cracks. Rep. E39, Brown University (AD-653716), May 1967.

TABLE I. - DIMENSIONLESS ELASTIC x-DIRECTIONAL STRESSES σ_x/σ_0 AND y-DIRECTIONAL STRESSES σ_y/σ_0 ALONG x-AXIS ($\tilde{y} = 0$) IN THE VICINITY OF THE NOTCH FOR A SPECIMEN WITH A SINGLE EDGE NOTCH SUBJECTED TO PURE BENDING

[Dimensionless load $\tilde{q} = 1.0$.]

(a) Dimensionless notch depth $\tilde{a} = 0.2$

x/a	Notch angle, α, deg		
	10	30	60
	$\hat{\sigma}_x$		
0.01	7.13	7.04	6.28
.02	5.01	4.93	4.47
.04	3.47	3.43	3.15
.06	2.77	2.75	2.56
.10	2.07	2.06	1.94
.20	1.35	1.35	1.29
	$\hat{\sigma}_y$		
0.01	7.40	7.44	7.36
.02	5.27	5.27	5.24
.04	3.73	3.72	3.71
.06	3.04	3.03	3.03
.10	2.33	2.27	2.33
.20	1.61	1.60	1.61

(b) Dimensionless notch depth $\tilde{a} = 0.3$

x/a	Notch angle, α, deg			
	3	10	30	60
	$\hat{\sigma}_x$			
0.01	7.72	7.88	7.66	6.72
.02	5.45	5.54	5.33	4.80
.04	3.80	3.85	3.72	3.40
.06	3.06	3.09	3.00	2.77
.10	----	2.30	2.26	2.11
.20	----	1.51	1.50	1.42
	$\hat{\sigma}_y$			
0.01	7.81	7.99	7.84	7.81
.02	5.54	5.65	5.52	5.54
.04	3.88	3.95	3.86	3.89
.06	3.13	3.18	3.10	3.14
.10	----	2.39	2.33	2.37
.20	----	1.54	1.51	1.54

TABLE I. - Continued. DIMENSIONLESS ELASTIC x-DIRECTIONAL STRESSES σ_x/σ_0 AND y-DIRECTIONAL STRESSES σ_y/σ_0 ALONG x-AXIS ($\tilde{y} = 0$) IN THE VICINITY OF THE NOTCH FOR A SPECIMEN WITH A SINGLE EDGE NOTCH SUBJECTED TO PURE BENDING

[Dimensionless load $\tilde{q} = 1.0$.]

(c) Dimensionless notch depth $\tilde{a} = 0.4$

x/a	Notch angle α, deg		
	10	30	60
	∂_x		
0.01	8.82	8.55	7.53
.02	6.24	6.07	5.40
.04	4.36	4.26	3.84
.06	3.51	3.44	3.13
.10	2.63	2.59	2.39
.20	1.70	1.68	1.58
	∂_y		
0.01	8.74	8.73	8.66
.02	6.13	6.13	6.11
.04	4.23	4.23	4.25
.06	3.36	3.36	3.39
.10	2.45	2.45	2.48
.20	1.44	1.44	1.47

(d) Dimensionless notch depth $\tilde{a} = 0.5$

x/a	Notch angle, α, deg		
	10	30	60
	∂_x		
0.01	10.63	10.46	8.98
.02	7.54	7.42	6.44
.04	5.28	5.20	4.58
.06	4.24	4.19	3.72
.10	3.15	3.13	2.80
.20	1.96	1.94	1.79
	∂_y		
0.01	10.29	10.49	10.21
.02	7.17	7.29	7.15
.04	4.86	4.94	4.88
.06	3.79	3.85	3.82
.10	2.63	2.67	2.68
.20	1.30	1.32	1.35

TABLE I. - Concluded. DIMENSIONLESS ELASTIC x-DIRECTIONAL STRESSES σ_x/σ_0 AND y-DIRECTIONAL STRESSES σ_y/σ_0 ALONG x-AXIS ($\tilde{y} = 0$) IN THE VICINITY OF THE NOTCH FOR A SPECIMEN WITH A SINGLE EDGE NOTCH SUBJECTED TO PURE BENDING

[Dimensionless load $\tilde{q} = 1.0$.]

(e) Dimensionless notch depth $\tilde{a} = 0.6$

x/a	Notch angle, α, deg		
	10	30	60
∂_x			
0.01	13.80	13.46	11.59
.02	9.78	9.56	8.30
.04	6.80	6.68	5.87
.06	5.42	5.33	4.73
.10	3.94	3.88	3.50
.20	2.27	2.24	2.04
∂_y			
0.01	13.06	13.26	12.98
.02	8.96	9.11	8.99
.04	5.91	6.01	5.98
.06	4.46	4.53	4.54
.10	2.85	2.91	2.93
.20	.83	.88	.90

TABLE II. - ORDER OF STRESS SINGULARITY n AT THE TIP OF THE NOTCH FOR SPECIMENS WITH A SINGLE EDGE NOTCH SUBJECTED TO PURE BENDING AND BEHAVING ELASTICALLY

[Dimensionless load $\tilde{q} = 1.0$.]

Dimensionless notch depth, $\tilde{a} = \frac{a}{w}$	Notch angle, α, deg							
	3		10		30		60	
	Source							
	Present report	Reference 8	Present report	Reference 8	Present report	Reference 8	Present report	Reference 8
	Order of stress singularity at tip of notch, n							
0.2	------	[a]0.5000	0.4990	0.4999	0.4986	0.4985	0.4875	0.4878
.3	0.4999	↓	.4999	↓	.4978	↓	.4896	↓
.4	------		.5007		.4989		.4929	
.5	------		.4999		.4989		.4886	
.6	------		.4999		.5010		.4863	
.7	------	↓	.5010	↓	.5000	↓	------	↓

[a]Value obtained for $\alpha = 0^{\circ}$.

TABLE III. - DIMENSIONLESS ELASTIC PLANE-STRESS RICE'S INTEGRAL $\frac{JE}{\sigma_0^2 w}$ FOR A SPECIMEN WITH A 10° EDGE NOTCH SUBJECTED TO PURE BENDING

[Dimensionless load $\tilde{q} = 1.0$; Poisson's ratio $\mu = 0.33$.]

Dimensionless notch depth, $\tilde{a} = \frac{a}{w}$	Dimensionless elastic plane-stress Rice's integral obtained	
	By integration of equation (21)	From stress intensity factor K_I in equation (20b)
0.3	1.193	1.212
.5	3.546	3.408

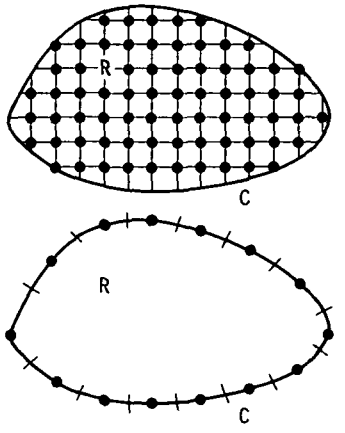

Figure 1. - Interior and boundary nodal points.

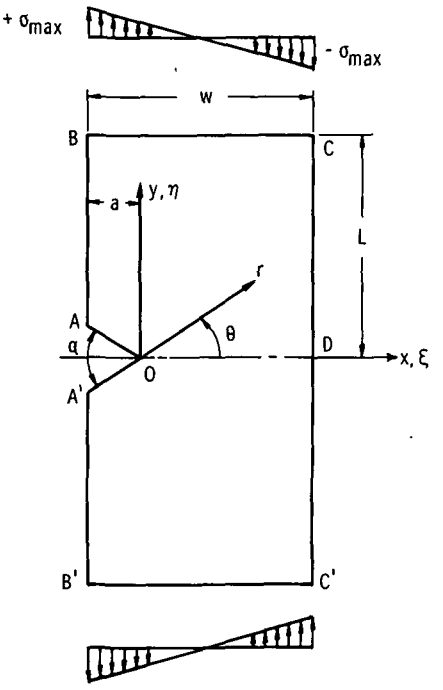

Figure 2. - Single-edge V-notched beam subject to pure bending load.

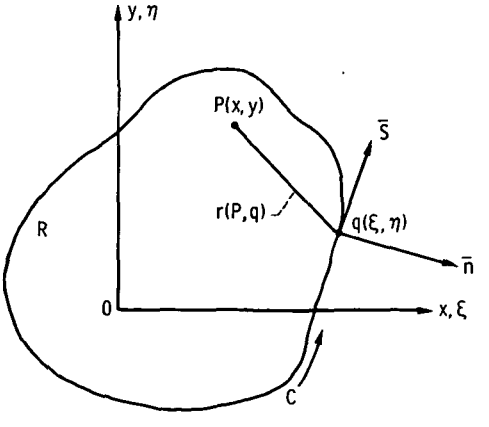

Figure 3. - Sign convention for a simply connected region R.

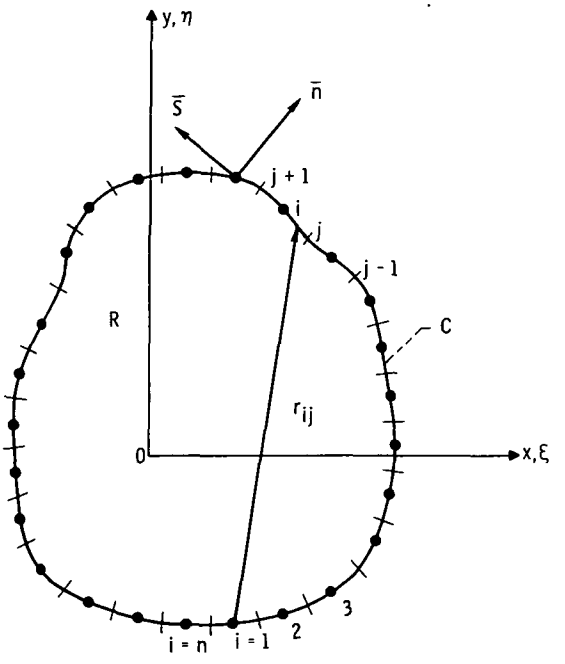

Figure 4. - Boundary subdivisions for P(x, y) ⊂ C.

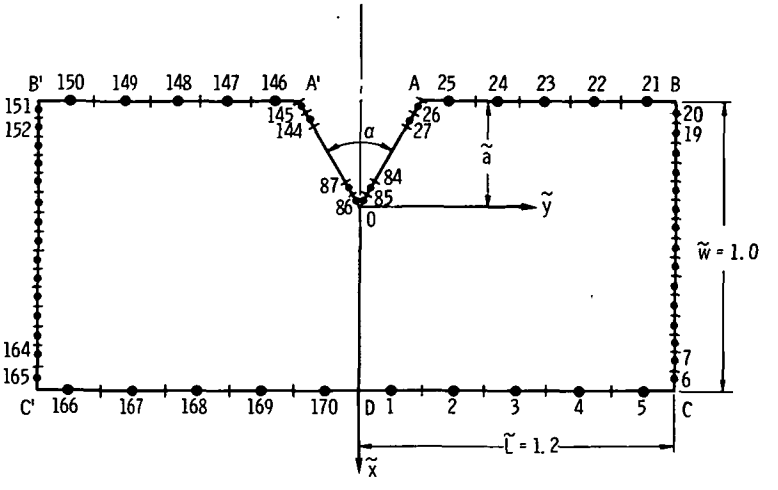

Figure 5. - Distribution of boundary subdivisions and nodal points.

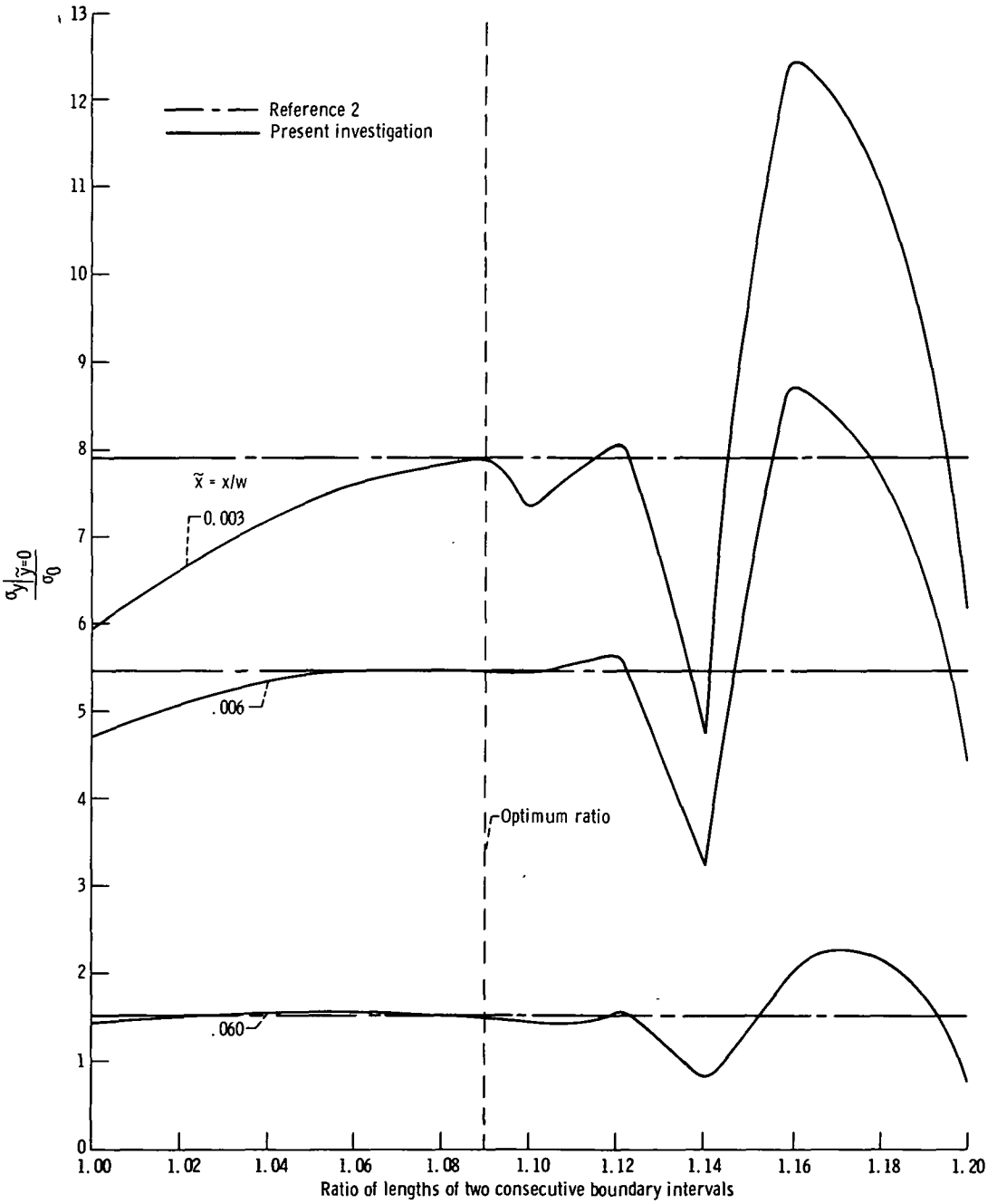

Figure 6. - Dimensionless elastic y-directional stress distribution in the vicinity of the tip of the notch for a specimen with a 10^0 edge notch and 60 tapered intervals along the notch. Dimensionless notch depth $\tilde{a} = 0.3$; dimensionless load $\tilde{q} = 1.0$.

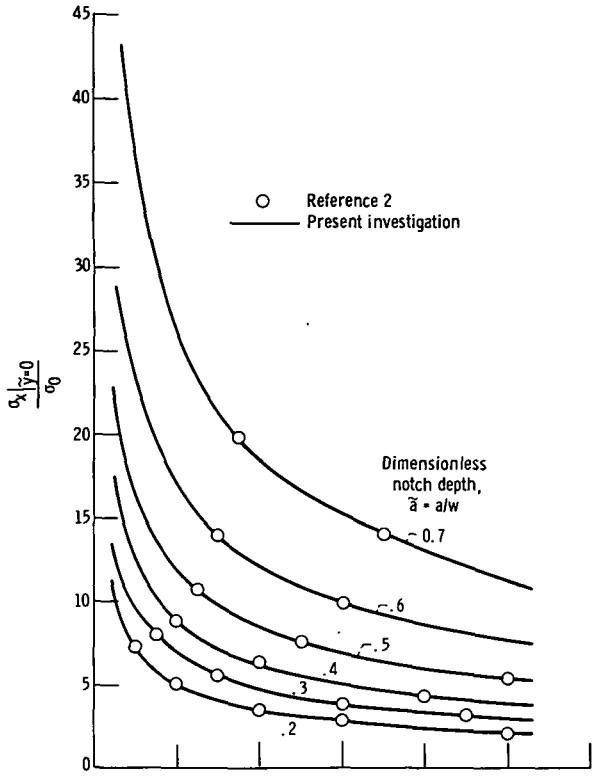

(a) Dimensionless x-directional stress as a function of $\tilde{x}$.

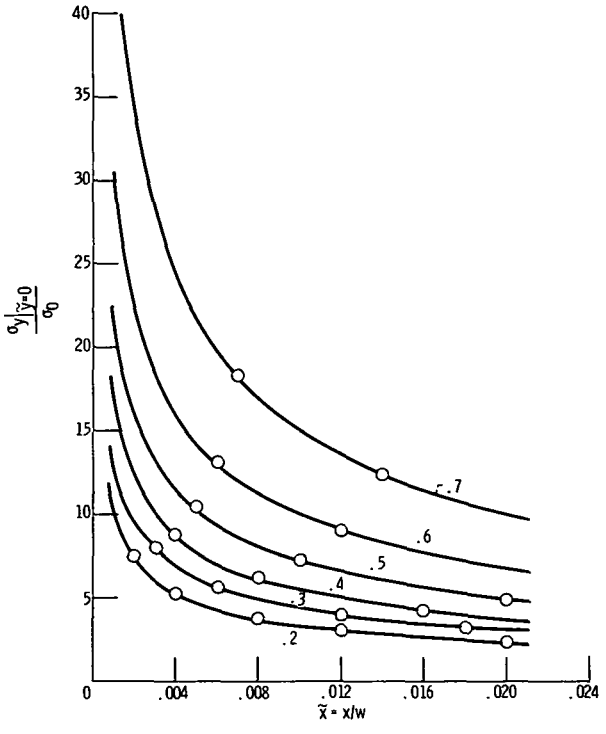

(b) Dimensionless y-directional stress as a function of $\tilde{x}$.

Figure 7. - Dimensionless elastic x-directional and y-directional stress distribution in the vicinity of the notch for a specimen with a 10^0 edge notch subjected to pure bending. Dimensionless load $\tilde{q}$ = 1.0.

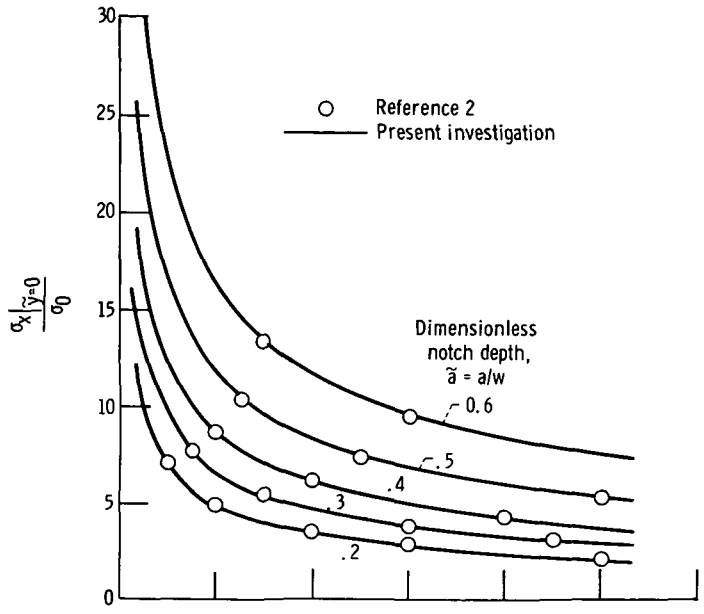

(a) Dimensionless x-directional stress as a function of $\tilde{x}$.

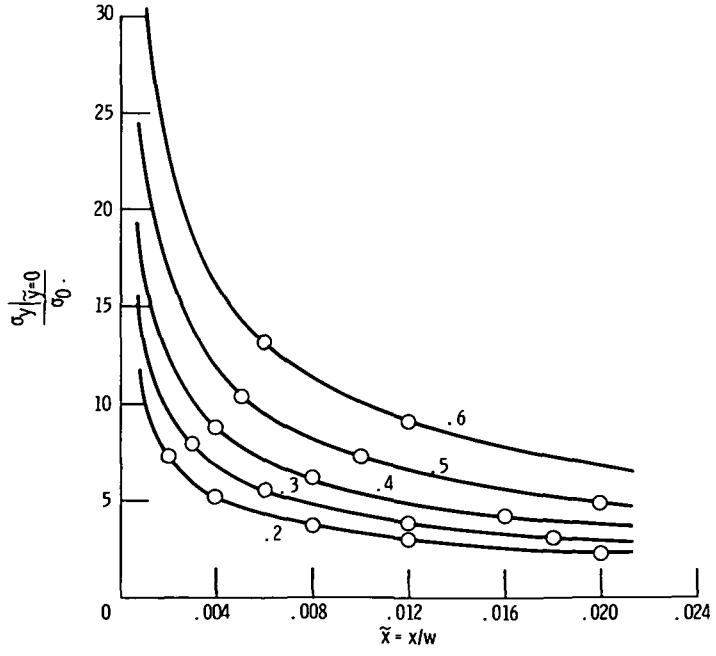

(b) Dimensionless y-directional stress as a function of $\tilde{x}$.

Figure 8. - Dimensionless elastic x-directional and y-directional stress distribution in the vicinity of the notch for a specimen with a 30^0 edge notch subjected to pure bending. Dimensionless load $\tilde{q} = 1.0$.

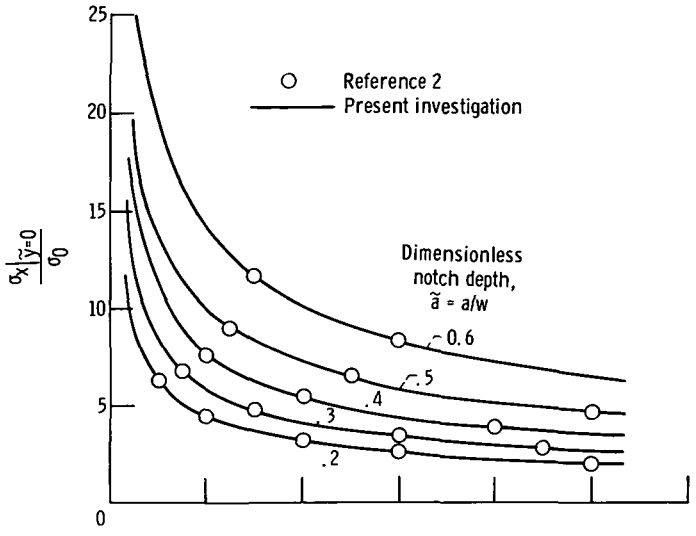

(a) Dimensionless x-directional stress as a function of $\tilde{x}$.

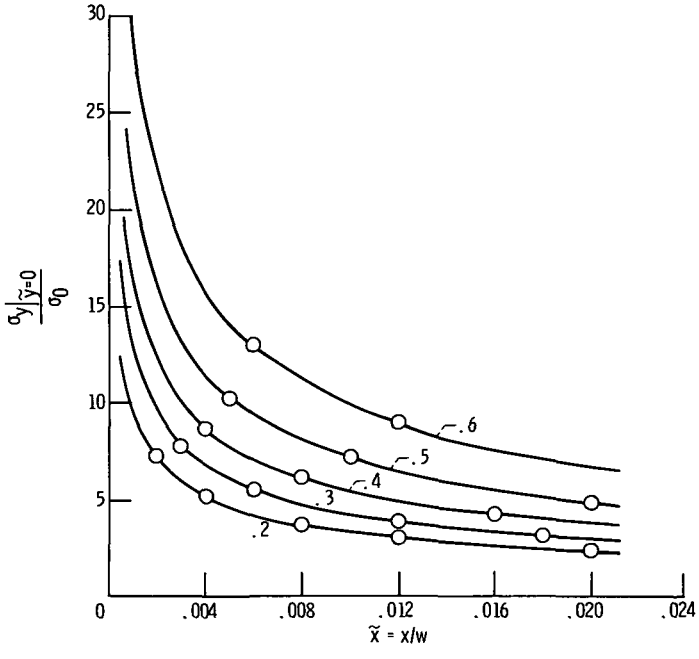

(b) Dimensionless y-directional stress as a function of $\tilde{x}$.

Figure 9. - Dimensionless elastic x-directional and y-directional stress distribution in the vicinity of the notch for a specimen with a 60^0 edge notch subjected to pure bending. Dimensionless load $\tilde{q}$ = 1.0.

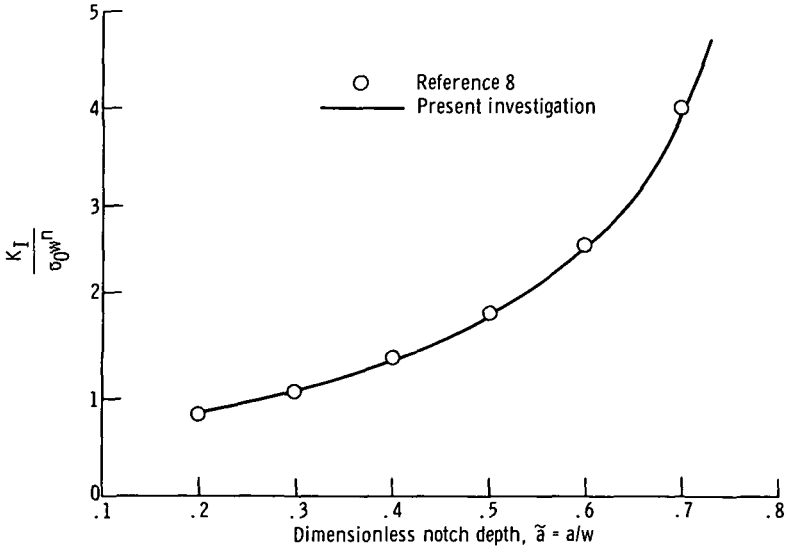

Figure 10. - Dimensionless stress intensity factor $\tilde{K}_I$ for a specimen with a 10^0 notch subjected to pure bending and behaving elastically. Dimensionless load $\tilde{q} = 1.0$.

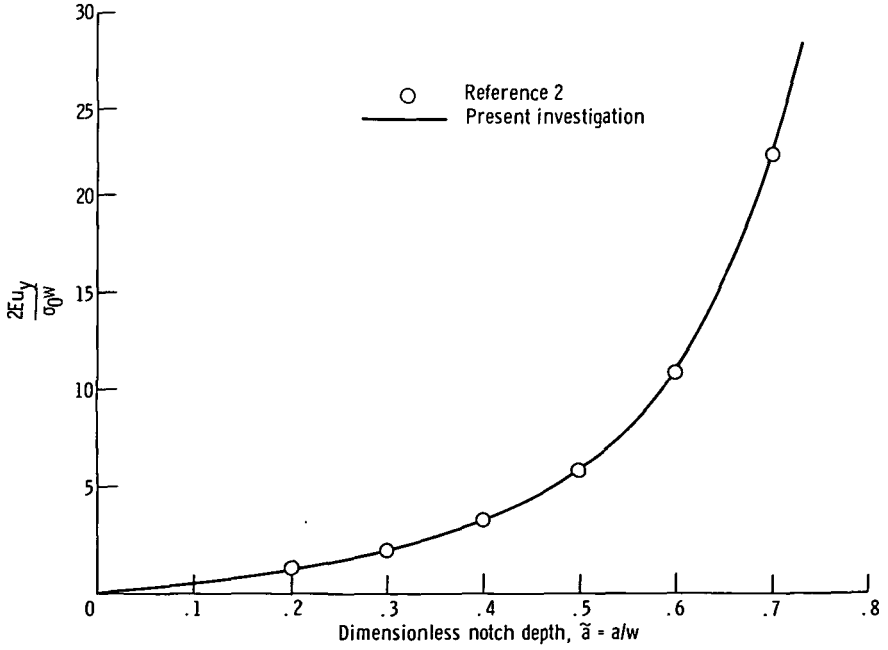

Figure 11. - Dimensionless elastic plane-stress y-directional notch opening displacement for a specimen with a 10^0 edge notch subjected to pure bending. Dimensionless load $\tilde{q} = 1.0$; Poisson's ratio $\mu = 0.33$.

NATIONAL AERONAUTICS AND SPACE ADMINISTRATION
WASHINGTON, D.C. 20546

OFFICIAL BUSINESS
PENALTY FOR PRIVATE USE $300

SPECIAL FOURTH-CLASS RATE BOOK

POSTAGE AND FEES PAID
NATIONAL AERONAUTICS AND SPACE ADMINISTRATION
451

U.S.MAIL

POSTMASTER: If Undeliverable (Section 158 Postal Manual) Do Not Return

"The aeronautical and space activities of the United States shall be conducted so as to contribute . . . to the expansion of human knowledge of phenomena in the atmosphere and space. The Administration shall provide for the widest practicable and appropriate dissemination of information concerning its activities and the results thereof."

—NATIONAL AERONAUTICS AND SPACE ACT OF 1958

NASA SCIENTIFIC AND TECHNICAL PUBLICATIONS

TECHNICAL REPORTS: Scientific and technical information considered important, complete, and a lasting contribution to existing knowledge.

TECHNICAL NOTES: Information less broad in scope but nevertheless of importance as a contribution to existing knowledge.

TECHNICAL MEMORANDUMS: Information receiving limited distribution because of preliminary data, security classification, or other reasons. Also includes conference proceedings with either limited or unlimited distribution.

CONTRACTOR REPORTS: Scientific and technical information generated under a NASA contract or grant and considered an important contribution to existing knowledge.

TECHNICAL TRANSLATIONS: Information published in a foreign language considered to merit NASA distribution in English.

SPECIAL PUBLICATIONS: Information derived from or of value to NASA activities. Publications include final reports of major projects, monographs, data compilations, handbooks, sourcebooks, and special bibliographies.

TECHNOLOGY UTILIZATION PUBLICATIONS: Information on technology used by NASA that may be of particular interest in commercial and other non-aerospace applications. Publications include Tech Briefs, Technology Utilization Reports and Technology Surveys.

Details on the availability of these publications may be obtained from:

SCIENTIFIC AND TECHNICAL INFORMATION OFFICE

NATIONAL AERONAUTICS AND SPACE ADMINISTRATION

Washington, D.C. 20546